Journal of Thermal Analysis, Vol. 30 (1985) 1227—1240

REVIEW OF SOME METALLURGICAL PROBLEMS SUITABLE FOR QUANTITATIVE CALORIMETRIC TREATMENT

J. Hertz

LABORATOIRE DE THERMODYNAMIQUE MÉTALLURGIQUE, FACULTÉ DES SCIENCES, U.A. C.N.R.S. 1108
UNIVERSITÉ DE NANCY I, B.P. 239
F-54506 VANDOEUVRE LES NANCY CEDEX, FRANCE

A review is given of various metallurgical problems treated in the author's laboratory, for which quantitative calorimetry gave very valuable information. Measurements of thermodynamic data for phase diagram calculations, vacancies in ordered alloys, annealing of steels, and the recovery and crystallization of amorphous alloys are successively examined.

Reflections on terminology and calorimetric methodology

Ten years ago our laboratory started working on thermodynamic studies of metallurgical materials, using in particular calorimetry, thermoanalysis, F.E.M. measurements and vapor pressure methods.

Today it has become difficult to distinguish between calorimetry and DTA. In most cases DTA also involves quantitative enthalpic determinations, using real calorimetric heat-flow meters, with an automatic treatment of the signal, giving the heat-flow directly in power units. Accordingly, we have made a distinction between real DTA and quantitative thermal analysis with linear variation of temperature, i.e. differential scanning calorimetry (DSC). In summary, quantitative calorimetry uses two different methods:

i — The calorimetric block is maintained at a constant temperature and during the experimental process a transformation takes place in the sample, which starts to pass from an initial well-defined state to a final well-reproducible state. With organic materials, for which the change of structural states is rather quick, this change of state can be promoted simply by introducing the sample into the cell at an initial temperature different from that of the cell. For liquid metallic materials, the situation is approximately the same. However, solid-state metallic materials are subject to very slow transitions, particularly at low temperatures. Hence, it is

Dedicated to Professor Dr Kurt Komarek on his 60th birthday.

John Wiley & Sons, Limited, Chichester
Akadémiai Kiadó, Budapest

dissolving the metallic sample in a solvent: an aqueous acid solvent or metallic bath. A systematic study of the literature leads us to conclude that the use of an acid aqueous solvent often induces a systematic error. In contrast, from our own experience we think that the use of a well-chosen metallic bath can be a very valuable method. In the next section we shall discuss an application of this method to calcium alloys. Another suitable method consists in obtaining very quick reactions between the mixed components, using high-temperature calorimetry. We illustrate this procedure with zirconium alloys, using one of our own calorimetric devices [1], acting up to 1800 K.

ii — Another way to obtain quantitative enthalpies of transition is to use a linear temperature variation of the cell during the experimental process (DSC). Such an increment of the temperature is able to create structural transformations. If the original state is an equilibrium one, and if all the intermediate states remain equilibrium states during the heating, the experimental curve will characterize all the equilibrium phase-transitions. In contrast, if the original state is a non-equilibrium state, increase of the temperature can allow us to observe the progressive return to equilibrium. Different types of experiments concerning the melting of stoichiometric compounds, the annealing treatment of hardenable steels and the recovery and the crystallization of amorphous alloys will illustrate these two kinds of DSC experiments.

It is important to note that there is no fundamental difference between the calorimeters suitable for isothermal and for non-isothermal enthalpimetry: for instance, a good heat-flow meter, such as the Calvet instrument, can also be used as an isothermal device or a DSC heat-flow meter.

Some examples of equilibrium experiments

Isothermal calorimetry using a liquid metallic bath

For several years we have been working on a systematic program to determine the thermodynamic properties of calcium alloys. Such alloys are often very sensitive to atmospheric corrosion, even at room temperature. Taking the compound $CaSn_3$ as an example, we can see (Fig. 1) from two different X-ray patterns that this compound is immediately decomposed by air at room temperature. For this reason, it is very useful to synthetize calcium alloys directly by reaction in the crucible of the calorimeter in purified argon. Figure 2 shows (after Bouirden and Notin) [2, 3] the integral enthalpy of formation of (Sn, Ca) alloys measured directly in a Calvet–Setaram device at 888 K. The experiment was carried out by adding small samples of pure calcium to a tin bath. The linear initial part of the curve

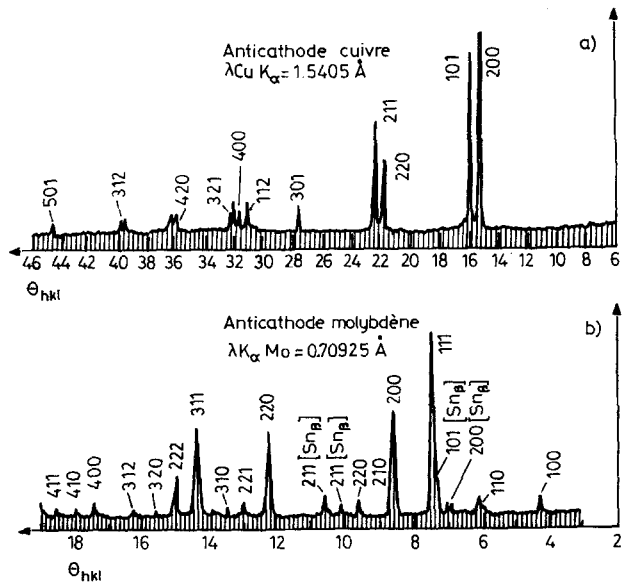

Fig. 1a X-ray pattern with $CaSn_3$ powder in an air atmosphere: the compound totally disappears with pure Sn crystallization at 20°C.

1b Same $CaSn_3$ powder in an argon atmosphere

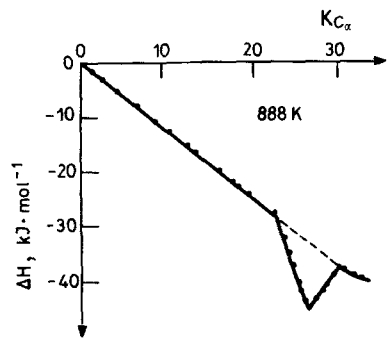

Fig. 2 Integral enthalpy of mixing of (Ca, Sn) alloys at 888 K: straight line pure liquid phase. Pic of enthalpy: precipitation and redissolution of $CaSn_3$ compound

corresponds to the homogeneous liquid mixture. Above 22 at.% calcium, $CaSn_3$ precipitates into the liquid bath and above 25 at.% calcium the same compound redissolves in a new 30 at.% Ca liquid phase. All the observed states in this experimental process are equilibrium states and we can deduce the enthalpy of formation of the compound directly: $\Delta h_f(Ca_{.25}Sn_{.75}$, solid, 888 K, references Caβ, Sn liquid) = 45.0 ± 0.1 kJ/mole

DSC measurements

To characterize the thermodynamic properties of this compound more completely, we set out to find its melting enthalpy and entropy. This research can be carried out in the same calorimeter if we stop the synthesis of the alloy just at the exact stoichiometry of the compound. The same Calvet calorimeter containing in one of its two cells, the pre-prepared compound $CaSn_3$ is now programmed for

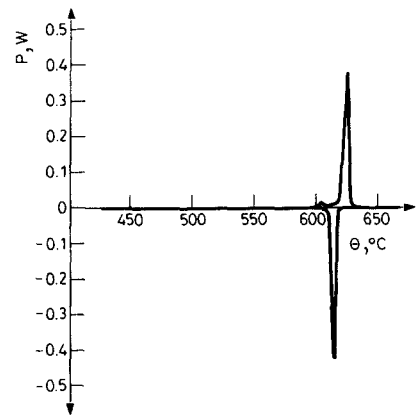

Fig. 3 Fusion and crystallization of about 3.5 g of $CaSn_3$ compound elaborated in the calorimeter. DSC experiment at 10 deg/h with Calvet's calorimeter

DSC. Figure 3 [2] shows the transcription in heat-flow power of the melting and crystallization curves obtained at a rate of 10 deg/h with about 3.5 g of the compound; the baseline was corrected using another experiment with an empty crucible. The heat flow and the temperature were recorded simultaneously by a microcomputer. The sensitivity curve of the calorimeter *vs.* temperature was included in the program of treatment. We obtained: ΔS melting $(Ca_{.25}Sn_{.75}) = 14.6 \pm 0.1$ J/mole degree; $T_m = 891 \pm 1$ K.

Isothermal high-temperature calorimetry

Let us choose another example of a directly operated alloying in the cell of the calorimeter with refractory alloys. Gachon [4–8] has studied the thermodynamic behavior of Ti and Zr with Fe, Co and Ni compounds, using a high-temperature heat-flow meter [1] working up to 1800 K. In an argon atmosphere, he prepared small pellets of fine powders of the components mixed in suitable proportions. The samples were introduced into the calorimeter at a temperature chosen just below the melting point of the desired compound. The alloying reaction can be very quick and the calorimetric signal gives the enthalpy of formation of the compound.

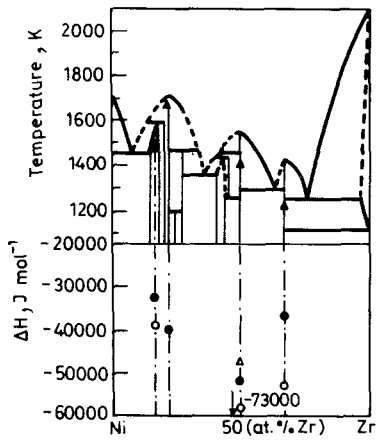

Fig. 4 Enthalpy of formation of 4 (Ni, Zr) compounds by high temperature.
▲ Calorimetry
● Gachon measurements [ref. 7]
○ Miedema's and Niessen's estimations [ref. 24]
△ Watson's and Bennett's estimations [ref. 25]

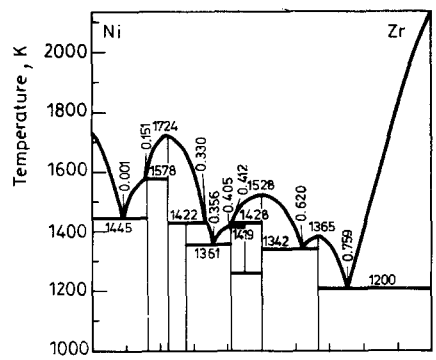

Fig. 5 After optimization of the thermodynamic data, phase diagram restitution of the NiZr system by Charles [ref. 9]

Taking the (Ni, Zr) system as an example, four compounds were synthetized by this method and the enthalpies obtained are reported in Fig. 4. An optimization calculation of the phase diagram, taking into account the four experimental enthalpies, was performed by Charles [9] and led to a good complete thermodynamic description of the system. Table 1 lists the thermodynamic properties for the seven compounds and also the liquid phase of the NiZr system. Figure 5 gives the calculated diagram.

Table 1 Thermodynamic restitution of the (Ni, Zr) system, reference states: Ni solid, Zrβ solid

Compounds						Biphased equilibrium				
x_{Zr}	$\frac{h^m}{J}$		s^m	T_{melt}/K		Nature	Temperature, K		X_{Zr}	
	Experiment	Calcul.		Experiment	Calcul.		Experiment	Calcul.	Experiment	Calcul.
0	0	0	0	1738	1738	Eutectic	1443	1445	0.088	0.091
0.17	−32,400	−36,200	−13.5		1580*	Peritectic	1573	1578	≃0.14	0.154
0.22	−39,500	−38,000	−12.5	1713	1724	Peritectic	1453	1422	≃0.33	0.336
0.276		−42,500	−15.0		1515*	Eutectic	1348	1361	0.360	0.356
0.412		−50,620	−19.5		1420*	Peritectic	1433	1419	≃0.41	0.406
0.45		−51,180	−19.8		1450*	Peritectic	1443	1428	≃0.425	0.412
0.50	−51,500	−52,330	−20.5	1543	1528	Eutegtic	1283	1342	0.635	0.620
0.67	−36,800	−37,500	−13.4	1413	1365	Eutectic	1233	1207	0.759	0.753
1	0	0	0	2128	2128					

*metastable melting

Application of equilibrium measurement results

For the phase diagram calculations, calorimetry gives the most suitable experimental data to determine the scale of the Gibbs functions. It is a well-known fact that multiplication of all the Gibbs energies of the different phases by the same factor will not change the phase diagram. Other experimental methods can also give Gibbs data directly, e.g. F.E.M. or mass-spectrography. We often combine calorimetric experiments with F.E.M. ones [10].

DSC calorimetry to characterize non-equilibrium states

Point defects: vacancies in ordered alloys

In a wide domain of concentration from 33 to 52 at.% Al, the $Fe_{1-x}Al_x$ alloys exhibit a long-range ordered structure with the B2 structure (CsCl isomorphism). After rapid quenching from high temperatures, these alloys remain perfectly ordered but many thermal vacancies become trapped in the network. The site concentration of vacancies can reach 2%, depending on the alloy stoichiometry and quenching temperature. These vacancies are not structural ones, because the number of vacant iron sites is always much higher than the number of vacant aluminium sites on both sides of the equiatomic concentration of alloys. Figure 6

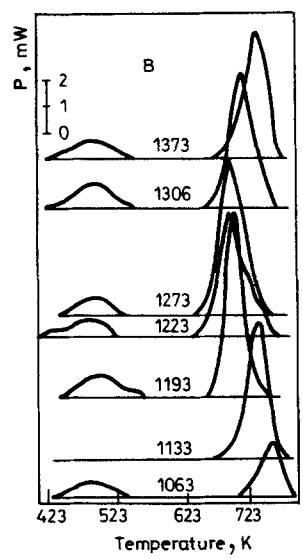

Fig. 6 DSC exothermal thermograms at the rate of 10 deg/h obtained with a Calvet's calorimeter using a $Fe_{.56}Al_{.44}$ quenched monocrystal: the first pic is linked with interstitial impurities. The second pic corresponds to the elimination of trapped vacancies [ref. 11]

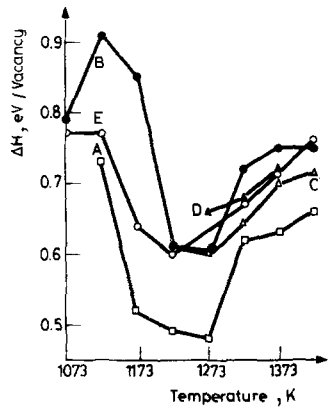

Fig. 7 Elimination enthalpy of one trapped vacancy for various $Fe_{1-x}Al_x$ alloys quenched at various temperatures $X_A = 0.40$, $X_B = 0.45$, $x_C = 0.49$, $x_D = 0.50$, $x_E = 0.51$ [ref. 11]

(after Lafi and Dirand) shows that heat power observed with a Calvet–Setaram calorimeter using a DSC procedure at a rate of about 10 deg/h, with a $Fe_{.55}Al_{.45}$ monocrystallized alloy quenched at different temperatures [11, 12]. The baseline is obtained by a second DSC heating after the initial annealing in the calorimeter. Two exothermic heat-flow peaks are observed. The sign of the heat flow exothermic for increasing temperature characterizes the return to the equilibrium state during the annealing process. The first peak is related to interstitial impurities trapped during the heating of the sample at high temperature. This peak does not appear for new high-purity monocrystals. The second peak corresponds to the process of elimination of vacancies through formation of a dislocation network. Similar experiments were carried out by Weber and Lesbats [12] by dilatometry on the same samples, and led to the concentration of vacancies in the quenched alloys. By coupling the two types of measurements, we can obtain the enthalpy of elimination of one vacancy. Figure 7 presents the variation of this energy with the stoichiometry of the alloy *vs.* the quenching temperature. To summarize the conclusions of this study, we have demonstrated that:

i — The elimination energy of these vacancies is of the same order of magnitude as for a pure or disordered metal.

ii — The variation of this energy with the quenching temperature corresponds to the diminution of preferential ordering of vacancies at the iron sites with increasing temperature. Some statistical models [13] can explain this ordering.

iii — We have to make a strong distinction between the formation and the elimination energy of vacancies, it is very easy to create a vacancy at the site of an aluminium atom in the wrong place, but the elimination of this vacancy brings back an iron atom to the site.

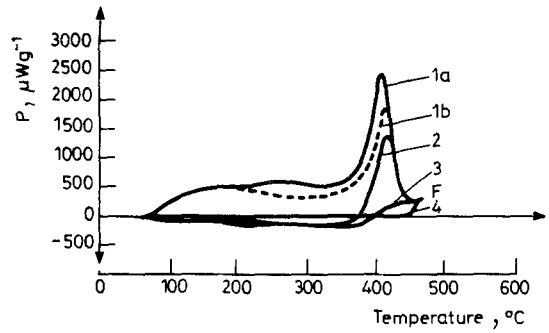

Fig. 8 DSC curves by annealing of AFNOR-61SC7 spring-steel.
1a) As oil-quenched. 1b) after immersion in liquid azot.
2) Pre-annealed up to η phase formation.
3) Pre-annealed up to χ carbide formation.
4) Pre-annealed up to θ formation.
"THERMANALYSE-CALORIMETER" at 30 deg/h [ref. 14 and 15]

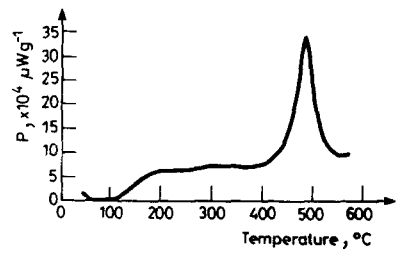

Fig. 9 DSC curve of the same oil quenched steel as in Fig. 8–1a but at the rate of 100 deg/mn.
"METTLER DSC 30-CALORIMETER" [ref. 16]

Annealing of hardenable steels

DSC studies allowed Godard, Akef and Hilger to follow the continuous transformation of spring-steels during the annealing process [16]. Two types of calorimeters were used, depending on the suitable rate of heating. For low rates such as 0.5 deg/min we used a Thermanalyse-Triflux device, and for high rates up to 100 deg/min a Mettler DSC 30. Fgures 8 and 9 show the DSC curves obtained with an Afnor-61SC7 steel after oil-quenching, during annealing at two different rates. Increasing the heating rate displaces the transitions to higher temperatures. All the heat flows are exothermic ones, corresponding to a non-equilibrium starting state. The most important points of this study are:

i — According to Dirand and Afqir [17], the annealing process always follows the same steps in the same sequence.

I) Precipitation of ε carbide, and progressive carbon transfer from the matrix to the carbide phase up to Fe_2C (with η ordered structure).

II) Transition of η carbide to Hägg's χcarbide $Fe_{2.5}C$ by diffusion of the atoms of the matrix.

III) Progressive transformation of the χ structure to the cementine structure $Fe_3C\Theta$.

ii — We have observed by DSC the transformation of the remaining austenitic phase, depending on the initial heat treatment (see curve 1b, Fig. 8).

iii — The thermal curves allow us to determine the kinetic process and the activation energy. As an example, step II of the transition corresponds to a one-order reaction with an activation energy of about 280.000 J/mole, corresponding to the diffusion of the matrix atoms. This step controls the kinetics of the industrial process.

Such laboratory studies can be transferred directly to industrial processes. In this particular case the annealing of springs can be shortened from 15 min to 2 min without alteration of the product.

Recovery and crystallization of amorphous alloys

Amorphous alloys can be obtained by various processes. Cunat [18, 19] has compared the thermodynamic behavior of different alloys produced by melt-spinning or by electrodeposition in aqueous solutions [20]. As an example, some melt-spun (Fe, B) alloys give the DSC curves in Fig. 10. Cunat used a DSC 111-

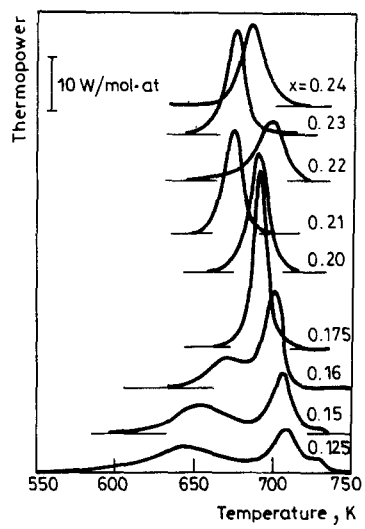

Fig. 10 Curves of the crystallization of $Fe_{1-x}B_x$ melt-spun glasses. "SETARAM DSC 111 calorimeter" at 3 deg/mn. Observe the double-pic crystallization up to $x<0.18$ at.% [ref. 19]

Setaram device at a rate of 3 deg/min. For $x_B < 0.18$ at.% B, he observed a double-peak crystallization process: first a pure iron phase crystallizes, the remaining amorphous phase containing about 0.22 at.% B. For $x_B > 0.18$ at.% B, the two steps can no longer be separated (percolation process). The total crystallization

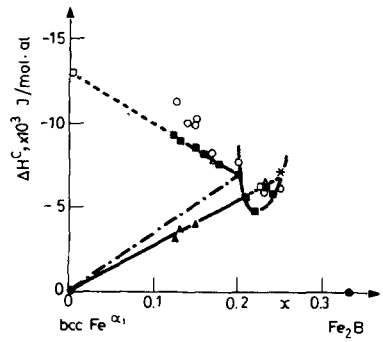

Fig. 11 ■ Total enthalpy of crystallization in $Fe_{1-x}B_x$ melt-spun glasses [ref. 19];
▲ Enthalpy of crystallization after iron phase pre-crystallization

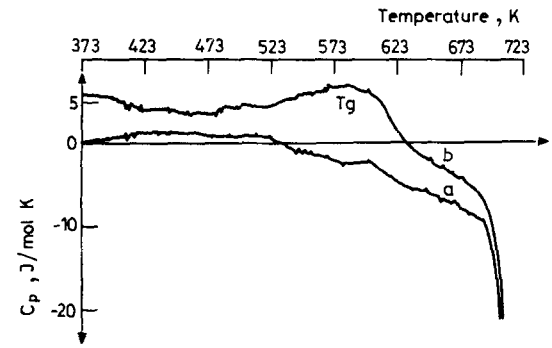

Fig. 12 Continuous C_p measurements with $Fe_{82.5}B_{17.5}$ melt-spun glasses at 3 deg/mn.
a) First annealing.
b) After an 8 days treatment at 500 K.
Observe the T_g endothermal effect near 573 K

enthalpy varies linearly with the concentration from 0 to 0.22 at.% B as for an equilibrium biphasic state (Fig. 11). These melt-spun alloys do not present any detectable excess heat flow during annealing up to the crystallization, taking as baseline the DSC curve obtained with the same sample after the crystallization. This fact indicates that, at a rate of 3 deg/min, no noticeable recovery takes place in this particular amorphous structure. Hence, we deduce that these alloys were initially in a structural state near the metastable state in the vicinity of the crystallization

temperature (700 K). This is the reason why the variation of the enthalpy *vs.* the concentration is linear, as for a real demixed liquid. However, using a very long isothermal pre-annealing at 500 K, we can displace the metastable equilibrium and the DSC curve (Fig. 12) now exhibits a rather sensitive endothermic *Tg* effect before the crystallization.

(Co, P) amorphous alloys were elaborated by electrodeposition in aqueous solutions [20]. These alloys [21] exhibit very unstable structural states with high

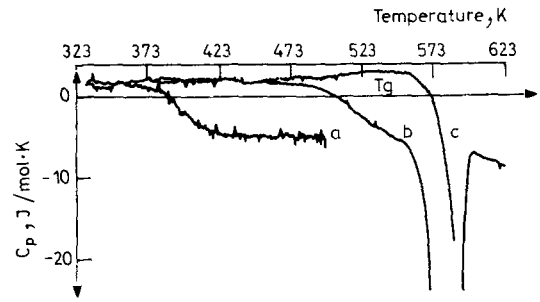

Fig. 13 Continuous C_p measurement obtained with a "SETARAM DSC 111" using an amorphous $Co_{82.5}P_{17.5}$ alloy prepared with aqueous electrodeposition.
a) First annealing at 3 deg/mn up to 500 K. Observe the important exothermal recovery.
b) Same sample second annealing.
c) Other sample 8 days treated at 500 K. Appearance of a T_g endothermal effect near 523 K

kinetics of recovery. On the first DSC heating, up to 500 K, we observe (Fig. 13a) an important exothermic heat flow corresponding to the recovery. After the cooling, the second DSC heating (curve b) no longer reveals any new recovery up to 500 K. Finally, after a long isothermal annealing (for 8 days) at 500 K and cooling, a new DSC curve no longer shows any recovery up to the crystallization (curve c), but we detect an endothermic effect near 550 K, corresponding to *Tg*. We have proposed [22] a statistical model of these processes using various order parameters. For each parameter there is an associated relaxation time, as in the Kovacs model [23].

Conclusion

We have reviewed various metallurgical problems treated in our laboratory by quantitative calorimetry, some of which can lead to industrial improvements. In the metallurgical field it is necessary to use for enthalpic measurements a large variety of thermal devices, covering a wide range of acting temperatures, from very low ones up to 1800 K (or more if possible), and also a large domain of heating rates,

from 0.2 to 100 deg/min. Several types of calorimeters may also operate as isothermal ones or as a DSC. The anisothermal technique is convenient for both equilibrium studies and studies of unstable and metastable states.

References

1 J. C. Gachon, M. Notin and J. Hertz, Proceedings JCAT Marseille — AFCAT, X (1979) HT 2.
2 L. Bouirden, Thèse de Doctorat de 3e cycle, Université de Nancy, I (1984) 75.
3 L. Bouirden, M. Notin and J. Hertz, Proceedings JCAT Bruxelles — AFCAT, XV (1984) 309.
4 J. C. Gachon, M. Notin and J. Hertz, Thermochim. Acta, 48 (1981) 155.
5 J. C. Gachon, J. Giner and J. Hertz, Scripta Met., 15 (1981) 981.
6 J. C. Gachon, M. Dirand and J. Hertz, J. Less-Common Metals, 85 (1982) 1.
7 J. C. Gachon and J. Hertz, Calphad, 7 (1983) 1.
8 J. C. Gachon, M. Dirand and J. Hertz, J. Less-Common Metals, 92 (1983) 307.
9 J. Charles, J. C. Gachon and J. Hertz, Calphad, 9 (1985) 21.
10 M. Notin, B. Djamshidi, J. C. Gachon and J. Hertz, An. Chim. Sciences des Matériaux, 6 (1981) 429.
11 H. Lafi, Thèse de 3e cycle, Université de Nancy, I (1982) 105.
12 H. Lafi, M. Dirand, L. Bouirden, J. Hertz, D. Weber and P. Lesbats, Acta Met. (1985). ted
13 D. Paris, Thèse de Doctorat ès Sciences, Université de Paris, VI (1979) 162.
14 J. P. Hilger, B. Godard, C. Cunat and J. Hertz, Acta Met., 31 (1983) 2095.
15 B. Godard, Thèse d'Université, Université de Nancy, I (1982) 95.
16 A. I. Akef, Thèse de 3e cycle, Université de Nancy, I (1984) 65.
17 M. Dirand and L. Afqir, Acta Met., 31 (1983) 1089.
18 C. Cunat, J. Charles, J. Hertz, J. M. Dubois and G. Le Caer, J. Phys. Colloque C9, 12, 43 (1982) 191.
19 C. Cunat, M. Notin, J. Hertz, J. M. Dubois and G. Le Caer, J. of Non-Crystalline Solids, 55 (1983) 45.
20 A. Obaïda, Thèse de 3e cycle, Université de Nancy, I (1982).
21 F. A. Kuhnast, F. Machizaud, J. Fléchon, C. Cunat and J. Hertz, Proceedings M.R.S.-Europe, Strasbourg, (1984).
22 C. Cunat and J. Hertz, Proceedings M.R.S.-Europe, Strasbourg, (1984).
23 A. J. Kovacs, J. M. Hutchinson and J. J. Aklonis, The structure of non-crystalline materials, Ph. Gaskell Editor, Taylor and Francis Publ. (1977) 153.
24 A. K. Niessen, F. R. de Boer, R. Boom, P. F. de Châtel, W. C. M. Mattens and A. R. Miedema, Calphad, 7 (1983) 51.
25 R. E. Watson and L. H. Bennett, Calphad, 5 (1981) 25.

Zusammenfassung — Es wird eine Übersicht über verschiedene, in unserem Laboratorium bearbeitete metallurgische Probleme gegeben, für die durch quantitative Kalorimetrie sehr genaue Informationen erhalten werden. Es wird auf Messungen thermodynamischer Daten für Phasendiagrammberechnungen, auf Fehlstellen in geordneten Legierungen, auf das Tempern von Stahl sowie auf Aufarbeitung und Kristallisation von amorphen Legierungen eingegangen.

Резюме — Представлено обозрение различных металлургических проблем, для решения которых количественная калориметрия дает очень точную информацию. Исследованы измерения термодинамических параметров для определения фазовой диаграммы, определения вакансий в упорядоченных сплавах закаленных сталей, регенерирование и кристаллизация аморфных сплавов.